# **Application of Chemical Reverse Engineering on Gun Propellant Composition Analysis: A Case Study**

Tsung-Mao Yang<sup>1\*</sup>, Shiau Shu Men<sup>2</sup>, Jin-Shuh Li<sup>1</sup>, Kai-Tai Lu<sup>1</sup>

# **ABSTRACT**

The purpose of this study is to propose a methodology that incorporates reverse engineering and chemical testing to accurately and efficiently analyze the composition of an unknown nitramine gun propellant, which will help to further develop the required formulation. First, the detailed geometric information of gun propellant sample was measured by optical microscopy. The components of the gun propellant sample were separated by the extraction characteristics of different solvents and then the separated components were analyzed qualitatively and quantitatively by means of X-Ray diffractometry, Fourier transform infrared spectroscopy, elemental analyzer, high performance liquid chromatography and high resolution gas chromatography-mass spectrometry. Finally, simultaneous thermogravimetry-differential scanning calorimetry and bomb calorimetry were used to confirm the composition analysis results of the gun propellant sample. The results of explosion heat measurement showed that the composition of the prepared propellant pellets was very similar to that of the original propellant pellets. Therefore, this chemical reverse engineering process was successfully used to determine the composition of the unknown nitramine gun propellant.

**Keywords:** reverse engineering, gun propellant, composition analysis, case study

# 逆向工程在火砲推進劑成分分析中的應用:一個案例研究

楊琮貿1\* 門孝書2 李金樹1 陸開泰1

<sup>1</sup>國防大學理工學院化學及材料工程學系 <sup>2</sup>國防大學理工學院化學工程碩士班

# 摘 要

本研究的目的是開發一種結合逆向工程和化學測試的方法,以準確有效地分析未知硝胺類發射藥的成分,這將有助於進一步開發所需的配方。首先,藉由光學顯微鏡量測發射藥樣品的幾何形狀及尺寸;然後,利用不同溶劑的萃取特性對發射藥樣品進行成分分離,再以 X 光繞射儀、傅立葉轉換紅外線光譜儀、元素分析儀、高效液相層析儀及高解析氣相層析質譜儀等儀器對分離後的成分進行定性和定量分析。最後,採用同步熱重-微差掃描熱卡計及燃燒彈熱卡計對發射藥樣品成分分析的結果進行確認。爆炸熱量測結果顯示,複製發射藥的組成非常接近原始發射藥。因此,此化學逆向工程程序成功用於確定未知硝胺類發射藥的組成。

關鍵詞:逆向工程、發射藥、成分分析、案例研究

<sup>&</sup>lt;sup>1</sup>Department of Chemical and Materials Engineering, Chung Cheng Institute of Technology, National Defense University

<sup>&</sup>lt;sup>2</sup>Master Program of Chemical Engineering, Chung Cheng Institute of Technology, National Defense University

文稿收件日期 112.04.07; 文稿修正後接受日期 112.09.01; \*通訊作者 Manuscript received Apr 07, 2023; revised Sep 01, 2023; \* Corresponding author

# I. INTRODUCTION

Reverse engineering (RE, also known as backwards engineering or back engineering) is a process that examines an existing product to determine detailed information and specifications in order to discover how it was made and how it works [1-3]. RE is applicable to the fields of computer engineering [4-5],mechanical engineering [6-8], design [9-11], electronic engineering [12-14], software engineering [15-17], chemical engineering [18-20] and systems biology [21-22]. In some cases, the only way to obtain the design of an original product is through RE. Product deformulation analysis, also known as chemical RE, is the process of identifying and/or quantifying one or more unknown chemical components of a formula. RE can help to understand which chemicals, substances or materials are incorporated into a product. Chemical RE involves mathematical modeling and experimentation. Many types of scientific and laboratory equipment can be used, including elemental analyzer (EA), spectrometers (MS, Raman, FTIR), nuclear magnetic resonance chromatographs (HPLC, (NMR), GC), microscopes, calorimeters, thermal analyzers (DSC, TGA) and mechanical testing equipment

Reverse innovative design has long been an important subject in the engineering field, which is a process of re-innovation on the existing system [23]. The knowledge gathered from reverse engineering can be incorporated to develop a new system, which bears some resemblance to the original system, but is not an exact copy. Reverse innovative design has gradually evolved as an important means of digestion and absorption of advanced technology. and has been applied in the optimal and innovative system designs as well as parts repairing of military and civilian products [24-26]. Sometimes, reverse engineering techniques are used to analyze the competitor's products in military or national security situations to improve one's own products [27].

The traditional gun propellants can be classified as single, double and triple base propellants according to their composition. The single-base propellants only contain nitrocellulose (NC) as the main energetic material. The double-base propellants contain NC infused with a liquid organic nitrate, such as

nitroglycerine (NG), which can gelatinize the NC. The triple-base propellants include the two compounds NC and NG of double-base propellants along with nitroguanidine (NQ). NQ can increase the energy content of the formulation without raising the flame temperature, which reduces the erosion of the gun barrel and also reduces muzzle flash [28-31]. However, traditional gun propellants are currently difficult to meet the requirements of modern artillery propellants. Therefore, the nitramine gun propellants have received extensive attention and research in recent years due to their excellent thermal properties, such as high energy, low detonation temperature, low average molecular weight of gas. The nitramine gun propellant can be prepared by adding energetic nitramine particles (RDX, HMX, etc.) to the single-based or double-based propellants [32-34]. propellants containing nitramine particles can increase the gunpowder power, and the erosion of the gun barrel is less [35]. Therefore, it is necessary to research and develop nitramine gun propellants based on military requirements.

In this study, the chemical RE was used to analyze the composition of an unknown nitramine gun propellant. First, the detailed geometric information of gun propellant sample was measured by optical microscopy (OM). Afterwards, the components of the gun propellant sample were separated by different solvents. The qualitative and quantitative analyses of each component were carried out by means of X-Ray diffractometry (XRD), Fourier transform infrared spectroscopy (FTIR), elemental analyzer (EA), high performance liquid chromatography (HPLC) and high resolution gas chromatography-mass spectrometry (HRGC-MS). In addition, thermogravimetry-differential simultaneous scanning calorimetry (STA TG-DSC) and bomb calorimetry (BC) were used to verify the results of the analysis. These research results will help to further develop the required formulation of the nitramine gun propellant.

#### II. EXPERIMENTAL

#### 2.1 Materials

The test sample of nitramine gun propellant of unknown composition was obtained from the arsenal in Taiwan as shown in Figure 1, which has actually been used in military applications. The certified reference standard samples of mixed explosive (Including 14 components such as HMX and RDX) and 3-Methyl-1,1-diphenylurea (Akardite II, C<sub>14</sub>H<sub>14</sub>N<sub>2</sub>O) used for HPLC analysis were purchased from Accustandard, Inc. (New Haven, CT, USA), and the catalog numbers are M-8330-R-0.5X and S-82930-0.1X, respectively. Camphor (1,7,7-Trimethylbicyclo[2.2.1] heptan-2-one,  $C_{10}H_{16}O$ ,  $\geq 99.0\%$ ) was analytical standard grade and purchased from Sigma Aldrich (St. Louis, MO, USA). HPLC grade methanol was also purchased from Sigma-Aldrich. Acetone (CH<sub>3</sub>COCH<sub>3</sub>, 99.8%) and methanol (CH<sub>3</sub>OH, 99.9%) were analytical grade and purchased from Sigma-Aldrich, which were used as solvents for dissolving the gun propellant sample. In addition, deionized water was used to dissolve the salt components in the gun propellant sample.



Fig.1. The sample of nitramine gun propellant of unknown composition from the arsenal in Taiwan

#### 2.2 Apparatus and procedures

First, the detailed geometric information of gun propellant sample was measured by using optical microscopy (OM). The composition analysis steps of gun propellant sample are shown in Figure 2 and described as follows:

(1) Acetone was used in the first extraction step of the gun propellant sample to dissolve the components in the gun propellant sample except for graphite and salt components. 0.3 g of gun propellant sample was weighed into a 250 ml round-bottom flask with 100 ml of acetone, and then the round-bottom flask was placed in an ultrasonic shaker for 1 hour to dissolve the gun propellant sample. Subsequently, the mixture was divided into acetone-soluble fraction and acetone-

- insoluble fraction by using 0.22  $\mu m$  PTFE syringe filters (Merck Millipore, Ltd., Taiwan).
- (2) The acetone-insoluble fraction obtained from the first extraction step was dried by a vacuum oven at 55°C for 1 hour to remove residual acetone and form a dry solid. The resulting dry solid contained graphite and salt components. Because graphite is insoluble in water and salt components are soluble in water. Therefore, deionized water was used as a solvent to dissolve the salt components of the dry solid. The resulting dry solid was weighed and added into a 250 ml round-bottom flask with 100 ml of deionized water, and then the salt components were completely dissolved in water under stirring. Subsequently, the mixture was divided into water-soluble fraction and water-insoluble fraction by using 0.22 µm PTFE syringe filters. The watersoluble fraction was placed in a rotary vacuum concentrator at 65°C to evaporate water and form dry salt crystals. The water-insoluble fraction was dried by a vacuum oven at 55°C for 1 hour to remove residual water, and weighed. Finally, the separated compounds were identified by means of X-Ray diffractometry (XRD, Bruker D2 Phaser).
- (3) The acetone-soluble fraction obtained from the first extraction step was placed in a rotary vacuum concentrator at 45°C to evaporate acetone and form a dry solid. Because nitrocellulose (NC) is insoluble in methanol. Therefore, methanol was used as the solvent in the second extraction step of the gun propellant sample to separate the NC. The resulting dry solid was weighed and added into a 250 ml round-bottom flask with 100 ml of methanol, and then the dissolvable components were completely dissolved in methanol under stirring. Subsequently, the solution was filtrated by using advantec 5C filter paper, and it was divided into methanolsoluble fraction and methanol-insoluble fraction.
- (4) The methanol-insoluble fraction obtained from the second extraction step was dried by a vacuum oven at 55°C for 24 hour to remove residual methanol. The obtained compound was identified by means of Fourier transform infrared spectroscopy (FTIR, PerkinElmer Spectrum 100), and elemental analyzer (EA, Elementar vario EL cube).

(5) The methanol-soluble fraction obtained from the second extraction step was analyzed and identified by using high performance liquid chromatography (HPLC, Jasco LC-4000 series) and high resolution chromatography-mass spectrometry (HRGC-MS, Joel AccuTOF GCx). HPLC analysis used a LiChrospher RP-18 column (5 µm, 250 cm×4.6 cm i.d.), a mobile phase system of methanol/water (50:50 v/v), a UV detection wavelength at 210 nm, a flow rate of 1.0 ml/min and an injection volume of 20 µL. HRGC-MS analysis used a Rxi<sup>TM</sup>-5ms column  $(0.25 \mu m, 30 \text{ m} \times 0.25 \text{ mm i.d.})$ . The temperatures of injector and detector were maintained at 230°C and 250°C, respectively. Methanol was used as blank. The split mode ratio of 50:1 was applied for the injection of a 1.0 μL sample. Helium was used as the carrier gas at a flow rate of 1.0 mL/min.

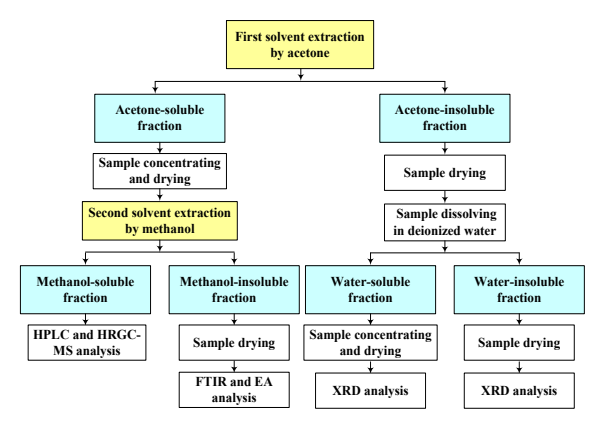


Fig.2. The composition analysis steps of gun propellant sample

In addition, the gun propellant sample was frozen in liquid nitrogen and then crushed using a copper mortar and pestle. The crushed powder was used for simultaneous thermogravimetrydifferential scanning calorimetry (STA TG-DSC, Netzsch STA 449 F3 Jupiter®) analysis to confirm the composition analysis results of the propellant sample. STA **TG-DSC** measurement was carried out in a nitrogen atmosphere at a heating rate of 10°C min<sup>-1</sup> using the sample weight in the range of 1.0-2.0 mg. The formula obtained from the composition analysis of the gun propellant sample was further used to prepare the propellant pellets. There were ten steps to prepare the propellant pellets, such as: (1) treating of the ingredients, (2) precise weighing, (3) wet mxing (NC, RDX, HMX, akardite II, K<sub>2</sub>SO<sub>4</sub> and ethanol-ether solution), (4) pressing, (5) cutting, (6) water cooking, (7) drying, (8) coating (camphor-ethanol solution), (9) final drying, (10) glazing (graphite). The explosion heats of the original and prepared propellant pellets were measure by bomb calorimetry (BC, Parr 6200) in a nitrogen atmosphere and the results were compared to confirm the composition analysis results of the gun propellant sample.

# III. RESULTS AND DISCUSSION

#### 3.1 Shape and size of gun propellant sample

Through visual observation, it was seen that the gun propellant sample was seven-perforated cylindrical pellets. The detailed geometric information was measured by OM, as shown in Figure 3. The diameter, length, inner web thickness and hole diameter of the seven-perforated cylindrical pellet are 2.08 mm, 1.86 mm, 664.1 µm and 68.7 µm, respectively.

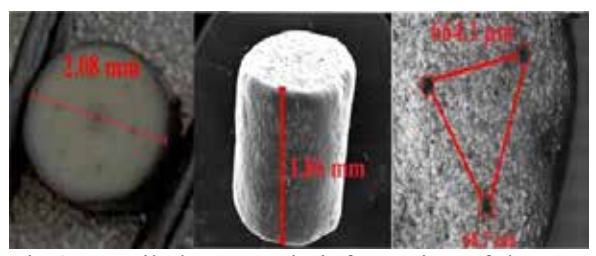


Fig.3. Detailed geometric information of the gun propellant sample.

# 3.2 Composition analysis of gun propellant sample

# 3.2.1 Acetone-insoluble fraction of first extraction step

The acetone-insoluble fraction of first extraction contained graphite and components, and was separated by using deionized water. The separated compounds were identified by means of XRD. Figure 4 shows the XRD pattern of the water-insoluble fraction. The three main peaks situated at 26.5°, 44.4° and 54.5° can be respectively assigned to the (002), (101) and (004) planes of graphite (JCPDS No. 41-1487). The analysis of the XRD pattern is similar to the report of Wang et al. [36]. Therefore, this analysis result can verify that the waterinsoluble fraction is graphite. Graphite is usually

coated on the surface of gun propellant pellets to prevent static electricity sparks from causing undesired ignitions [37]. The XRD pattern of the water-soluble fraction is shown in Figure 5. The main peaks located at 17.6°, 21.4°, 23.9°, 29.8°, 30.8°, 35.7°, 37.1°, 48.1°, 54.6°, 62.8° and 75.4° can be respectively assigned to the (200), (210), (020), (121), (301), (002), (400), (040), (303), (621) and (404) planes of K<sub>2</sub>SO<sub>4</sub> crystals (JCPDS No. 24-0703). The analysis of the XRD pattern is similar to the report of Al-Dhahir et al. [38]. Therefore, this analysis result can confirm that the salt component of the water-soluble fraction is K<sub>2</sub>SO<sub>4</sub> crystals. K<sub>2</sub>SO<sub>4</sub> is used in gun propellant formulations to suppress muzzle flash by preventing the ignition of fuel rich combustion gases that are expelled out of the gun barrels [39]. Graphite and K<sub>2</sub>SO<sub>4</sub> were individually weighed after drying to determine their content in the gun propellant sample. The weighing results indicate that the weight ratios of graphite and K<sub>2</sub>SO<sub>4</sub> are 1.0% and 1.4%, respectively.

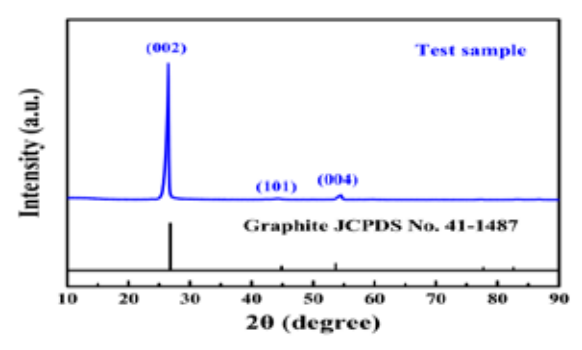


Fig.4. XRD pattern of the water-insoluble fraction

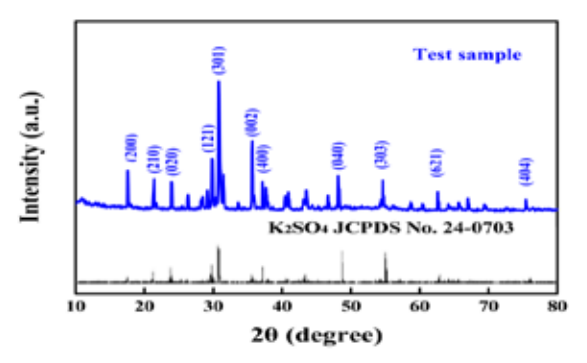


Fig.5. XRD pattern of the water-soluble fraction

# 3.2.2 Methanol-insoluble fraction of second extraction step

It was predicted that the methanol-insoluble

fraction of second extraction was NC. The separated compound was identified by means of FTIR and EA. Figure 6 shows the FTIR spectrum of the methanol-insoluble fraction. -NO<sub>2</sub> symmetric and asymmetric stretching vibrations are respectively found at 1270 and 1650 cm<sup>-1</sup>, and rocking and scissoring vibrations are found at 760 and 860 cm<sup>-1</sup>, respectively. C-O stretching vibration is observed in the region of 1002-1064 cm<sup>-1</sup>. In addition, -CH stretching vibration is found at 2840 cm<sup>-1</sup>. It is worth noting that the weak stretching vibration of -OH appears at 3500 cm<sup>-1</sup>. This means that a small amount of OH groups are not replaced by NO<sub>2</sub> groups during the nitration process of cellulose. These analysis results are similar to the report of Costa et al. [40]. Therefore, the FTIR spectrum can verify that the methanol-insoluble fraction is NC. Furthermore, the elemental composition of the separated NC was analyzed by EA. The experiment was run three times and the average value of each element content was calculated as shown in Table 1. The analysis result shows that the separated NC contains 13.47% nitrogen (N), 25.27% carbon (C), 2.62% hydrogen (H) and 58.64% oxygen (O), which are very close to the theoretical values of NC composition (14.14% N, 24.24% C, 2.36% H and 59.26% O). Among them, the H content is slightly higher and the N and O contents are slightly lower in the separated NC, which may be because a small amount of OH groups are not replaced by NO<sub>2</sub> groups during the nitration process of cellulose. The separated NC has a nitrogen content of 13.47%, NC belongs to Grade B, Type I, according to the US Military Standard MIL-DTL-244C. The weighing result indicates that the weight ratio of NC in the gun propellant sample is 67.4%.

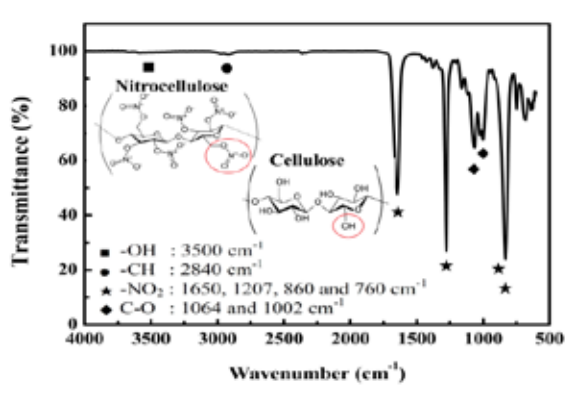


Fig.6. FTIR spectrum of the methanol-insoluble fraction

Table 1. Elemental analysis of separated NC

Molecular formula $[C_6H_7O_2(ONO_2)_3]_n$					
Element	Test 1	Test 2	Test 3	Average value	Theoretica l value
N (wt.%)	13.48	13.45	13.47	13.47	14.14
C (wt.%)	25.34	25.25	25.22	25.27	24.24
H (wt.%)	2.62	2.61	2.62	2.62	2.36
O (wt.%)	58.56	58.69	58.69	58.64	59.26

# 3.2.3 Methanol-soluble fraction of second extraction step

The methanol-soluble fraction of second extraction was analyzed by means of HPLC and HRGC-MS. Figure 7 displays the HPLC chromatogram of the methanol-soluble fraction. Five well-separated peaks are found at retention time of 1.627 min (component A), 2.946 min (solvent), 4.946 min (component B), 8.530 min (component C) and 21.145 min (component D). Compared with the HPLC chromatogram of the M-8330-R-0.5X standard sample shown in Figure 8, components B and C can be identified as nitramine explosives HMX and RDX, respectively. **HRGC-MS** analysis of the methanol-soluble fraction reveals two components. Through analysis MS and identification, these two compounds camphor (molecular weight 152) and Akardite II (molecular weight 226), as shown in Figure 9 and Figure 10. The chemical structures are presented as insets in the figures. In addition, the standard sample solutions of camphor and Akardite II were prepared for HPLC analysis and compared with the HPLC chromatogram of the methanol-soluble fraction shown in Figure 7. Figure 11 presents the comparison of HPLC chromatograms of camphor standard sample and methanol-soluble fraction, component A can be identified as camphor. Camphor can be used in gun propellant formulations as a burn rate modifier. The comparison of HPLC chromatograms of Akardite II standard sample and methanol-soluble fraction is given in Figure 12, component D can be identified as Akardite II. Akardite II can be used in gun propellant formulations as a stabilizer.

Four calibration lines were prepared to determine the contents of camphor (component A), HMX (component B), RDX (component C) and Akardite II (component D) in the gun propellant sample, as shown in Figure 13. The analysis results indicate that the weight ratios of camphor, HMX, RDX and Akardite II are 2.8%, 1.4%, 22.6% and 1.1% in the gun propellant sample, respectively.

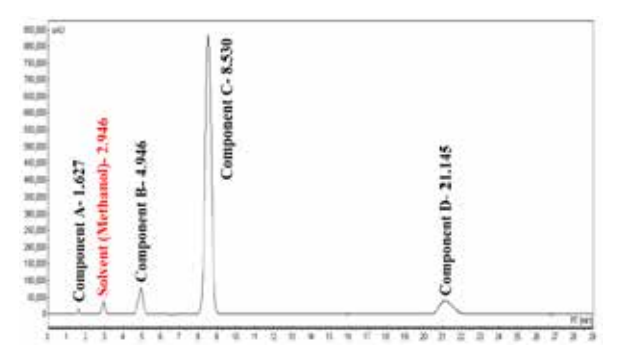


Fig.7. HPLC chromatogram of the methanol-soluble fraction

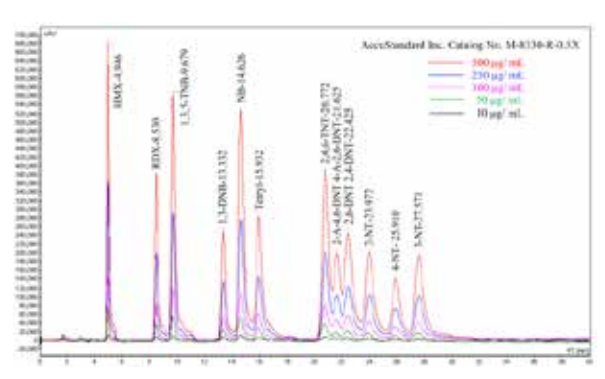


Fig.8. HPLC chromatogram of M-8330-R-0.5X standard sample

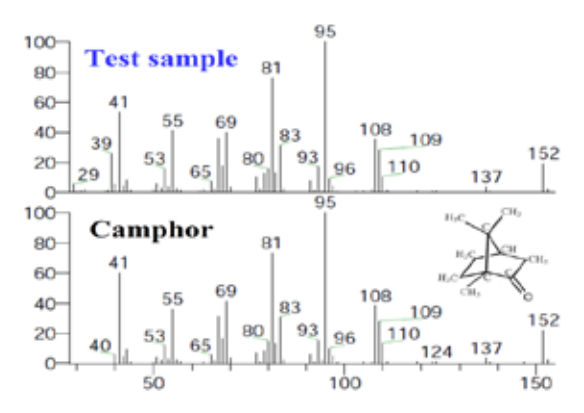


Fig.9. MS analysis and identification for camphor component

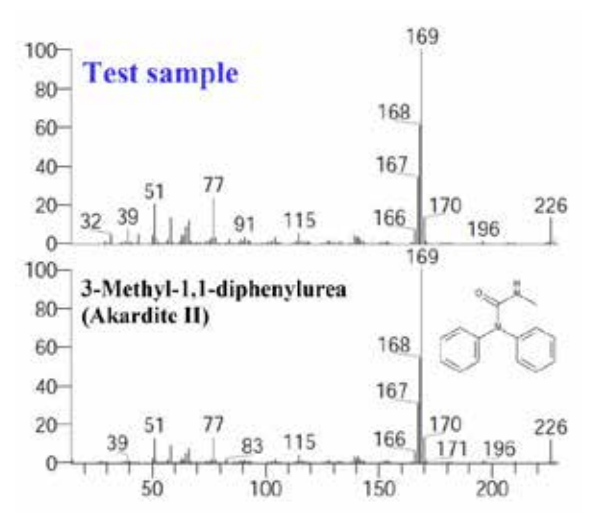


Fig.10. MS analysis and identification for Akardite II component

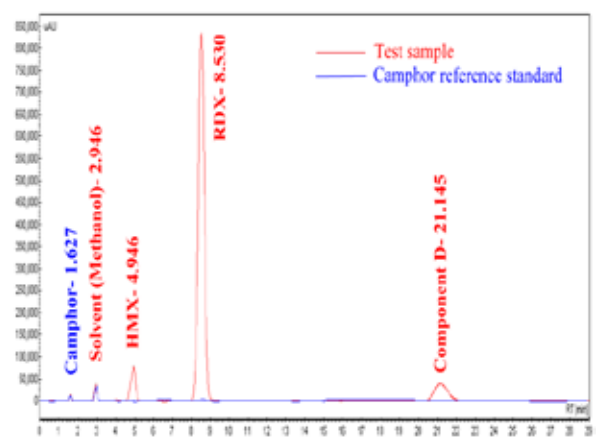


Fig.11. The comparison of HPLC chromatograms of camphor standard sample and methanol-soluble fraction

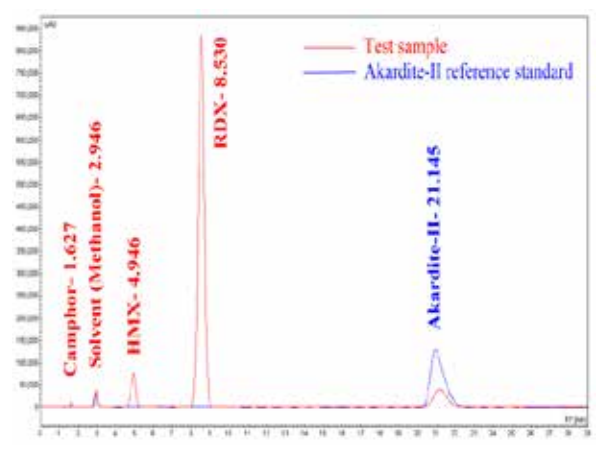


Fig.12. The comparison of HPLC chromatograms of Akardite II standard sample and methanol-soluble fraction

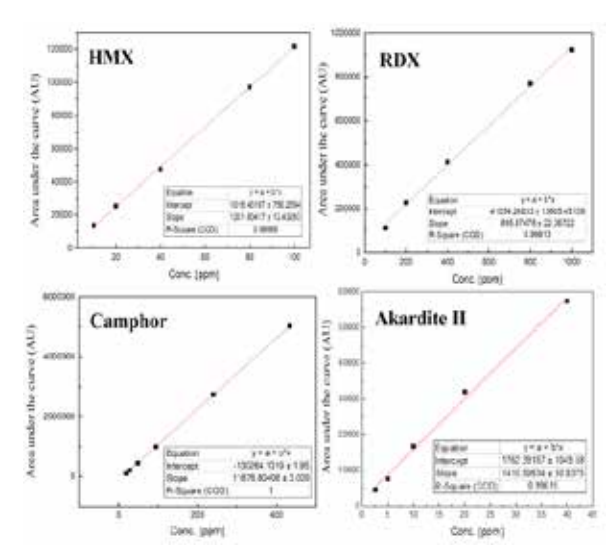


Fig.13. The calibration lines of HMX, RDX, camphor and Akardite II

# 3.2.4 Integration of qualitative and quantitative analysis

The results of the qualitative and quantitative content analysis of the gun propellant sample are summarized in Table 2. The results of quantitative content analysis show that the total amount of all compounds in the gun propellant sample is only about 97.7%. The remaining 2.3% content in the gun propellant sample can be reasonably considered to be the moisture on the sample surface and the residual solvent in the sample.

Table 2. Results of qualitative and quantitative content analysis of gun propellant sample

Content of gun propellant sample					
Compound	Weight ratios (%)				
graphite	1.0				
$K_2SO_4$	1.4				
NC	67.4 (N content 13.47%)				
camphor	2.8				
HMX	1.4				
RDX	22.6				
Akardite-II	1.1				
Total	97.7				

# 3.3 Verification analysis of gun propellant sample

### 3.3.1 TG-DSC analysis

The gun propellant sample was frozen in liquid nitrogen and then crushed using a copper mortar and pestle. The crushed powder was used for STA TG-DSC analysis to confirm the composition analysis results of the gun propellant sample. Figure 14 shows DSC curve of gun propellant sample. Three connected exothermic peaks are observed in the range of 170-250°C, and one independent exothermic peak is observed between 260°C and 310°C. Celebioglu et al. [41] have reported that the decomposition temperature of camphor is about 178°C by DSC analysis. It has also been found by Cieslak et al. [42] that the decomposition temperature of NC & Akrdite II is about 203°C by DSC analysis. In addition, Jia et al. [43] have measured the decomposition temperatures of RDX and HMX by DSC analysis be approximately 243°C and 284°C, respectively. Therefore, in Figure 14, these four peak temperatures at 182°C, 203°C, 240°C and correspond to the decomposition temperatures of camphor, NC & Akrdite II, RDX and HMX, respectively. A weak endothermic peak is found near 100°C which is due to evaporation of moisture from the sample surface. The characteristic peaks of graphite and K<sub>2</sub>SO<sub>4</sub> do not appear in the DSC thermogram, because the initial reaction temperatures of graphite and K<sub>2</sub>SO<sub>4</sub> are around 750°C and above 1,000°C, respectively [44, 45]. Figure 15 shows the corresponding TG curve of gun propellant sample. The weight loss below 170°C is 2.3%, which can be attributed to the evaporation of moisture and residual solvent. The weight loss in the region 170-220°C is 71.3% due to the thermal decomposition of NC & Akrdite II and Camphor. The weight loss between 220 and 400°C is 24.0%, which should be attributed to the thermal decomposition of RDX and HMX. The residual weight is about 2.4% because of the presence of graphite and K<sub>2</sub>SO<sub>4</sub>, which have higher thermal stability. Based on the above TG-DSC analysis, the composition analysis results of the gun propellant sample have been successfully verified.

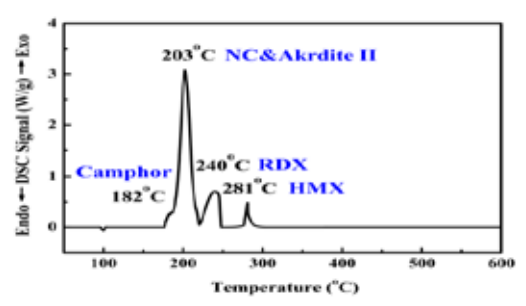


Fig.14. DSC curve of gun propellant sample

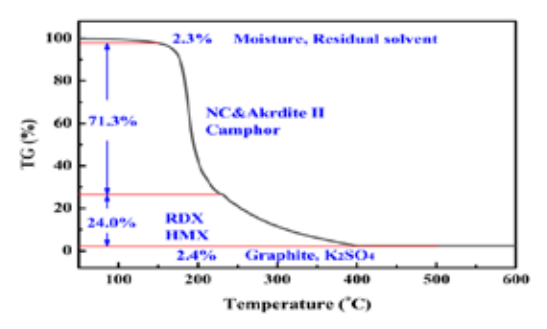


Fig.15. TG curve of gun propellant sample

### 3.3.2 Bomb calorimetry (BC) analysis

The explosion heats of the original and prepared propellant pellets were measure by bomb calorimetry (BC) in a nitrogen atmosphere and the results were compared to confirm the composition analysis results of the gun propellant sample. The experiment of each sample was repeated three times and the reported data is the average of these experiments. The experimental results of BC are listed in Table 3. It is found that the explosion heat of the prepared propellant pellets is 898.05 cal/g, which is very close to that of the original propellant pellets (894.25 cal/g). The difference between the both is only about 0.42%, which means that the composition of the prepared propellant pellets is very similar to that of the original propellant pellets.

Table 3. Experimental results of bomb calorimetry

Exp. No.	Explosion heat (cal/g)			
Ехр. №.	Original pellets	prepared pellets		
1	893.91	903.18		
2	898.90	893.67		
3	889.94	897.30		
Average value	894.25	898.05		

# IV. CONCLUSION

In this study, the chemical RE was successfully used to analyze the composition of unknown nitramine gun propellant. First, the components of the gun propellant sample were separated by the extraction characteristics of different solvents. Then the separated components were analyzed qualitatively and quantitatively by means of XRD, FTIR, EA, HPLC and STA TG-DSC. Finally, STA TG-DSC and BC were used to confirm the composition analysis results of the gun propellant sample. The verification results show that the explosion heat of the prepared propellant pellets is 898.05 cal/g, which is very close to that of the original propellant pellets (894.25 cal/g). The difference between the both is very small, which means that the composition of the prepared propellant pellets is very similar to that of the original propellant pellets. These analysis results will help to further develop the required formulation of the nitramine gun propellant.

# **ACKNOWLEDGEMENT**

The authors thank the 205<sup>th</sup> Arsenal in Taiwan for supplying experimental ingredients. The authors would also like to thank Professors Tsao-Fa Yeh and Chyi-Ching Hwang for their useful suggestions regarding data processing.

### REFERENCES

- [1] Stjepandic, J., Wognum, N., Verhagen, W. J. C. (Editor), Concurrent Engineering in the 21st Century Foundations, Developments and Challenges, Chapter 13: Reverse Engineering, Springer International Publishing, Switzerland, pp. 319-354, 2015.
- [2] Wang, W., Reverse Engineering-Technology of Reinvention, CRC press, New York, USA, pp. 1-20, 2011.
- [3] Thayer, K., How Does Reverse Engineering Work?, Engineering360, 2017. (https://insights.globalspec.com/article/7367/how-does-reverse-engineering-work)
- [4] Bi, Z. M., Wang, X. Q., Computer Aided Design and Manufacturing, Chapter 2: Computer Aided Reverse Engineering, John Wiley & Sons Ltd., New Jersey, USA, pp. 173-218, 2020.
- [5] Mancas, C., "Should Reverse Engineering

- Remain a Computer Science Cinderella?," Journal of Information Technology & Software Engineering, Article No. S5-e001, 2013.
- [6] Jain, V., Jain, S., Yadav, K., "FRE: Functional Reverse Engineering for Mechanical Components," International Journal of Advanced Mechanical Engineering, Vol. 4, No. 2, pp. 139-144, 2014.
- [7] Buonamici, F., Carfagni, M., Furferi, R., Governi, L., Lapini, A., Volpe, Y., "Reverse Engineering of Mechanical Parts: A Template-Based Approach," Journal of Computational Design and Engineering, Vol. 5, No. 2, pp. 145-159, 2018.
- [8] Pang, T. Y., Fard, M., "Reverse Engineering and Topology Optimization for Weight-Reduction of a Bell-crank", Applied Sciences, Vol. 10, Article No. 8568, 2020.
- [9] Fagette, P., "Reverse Engineering by Design: Using History to Teach." IEEE Pulse, Vol. 4, No. 1, pp. 33-38. 2013.
- [10] Sadiq, J., Waheed, T., "Reverse Engineering & Design Recovery: An Evaluation of Design Recovery Techniques," International Conference on Computer Networks and Information Technology, Abbottabad, Pakistan, pp. 325-332, 2011.
- [11] Philippow, I., Streitferdt, D., Riebisch, M., Naumann, S., "An approach for Reverse Engineering of Design Patterns," Software and Systems Modeling, Vol. 4, No. 1, pp. 55-70, 2005.
- [12] Erozan, A. T., Hefenbrock, M., Beigl, M., Aghassi-Hagmann J., Tahoori, M. B., "Reverse Engineering of Printed Electronics Circuits: From Imaging to Netlist Extraction," IEEE Transactions on Information Forensics and Security, Vol. 15, pp. 475-486, 2020.
- [13] Quadir, S. E., Chen, J. L., Forte, D., Asadizanjani, N., Shahbazmohamadi, S., Wang, L., Chandy, J., Tehranipoor, M., "A Survey on chip to System Reverse Engineering," ACM Journal on Emerging Technologies in Computing Systems, Vol. 3, No. 1, Article No. 6, 2016.
- [14] Torrance R., James, D., "Reverse Engineering in the Semiconductor Industry," Proceedings of the IEEE 2007 Custom Integrated Circuits Conference, California, USA, pp.429-436, 2007.
- [15] Hasbi, M., Budiardjo, E. K., Wibowo, W. C.,

- "Reverse Engineering in Software Product line A systematic literature Review," Proceedings of the 2018 2nd International Conference on Computer Science and Artificial Intelligence, Shenzhen, China, pp.174-179, 2018.
- [16] Moraga, M., Zhao, Y. Y., "Reverse Engineering a Legacy Software in a Complex System: A Systems Engineering Approach," INCOSE International Symposium Washington, Vol. 28, No. 1, pp. 1250-1264, 2018.
- [17] Aabidi, M. H., Mahi, B. E., Baidada, C., Jakimi, A., Ammar, H., "Benefits of Reverse Engineering Technologies in Software Development Makerspace," ITM Web of Conferences, Vol. 13, Article No. 01028, 2017.
- [18] Forrest, M. J., Rubber Analysis Characterisation, Failure Diagnosis and Reverse Engineering, 5. Reverse Engineering and Product Deformulation, De Gruyter, Berlin, Germany, pp. 129-154, 2019.
- [19] Wilding, M., Peat, T. S., Kalyaanamoorthy, S., Newman, J., Scott, C., Jermiin, L. S., "Reverse Engineering: Transaminase Biocatalyst Development Using Ancestral Sequence Reconstruction," Green Chemistry, Vol. 19, pp. 5375-5380, 2017.
- [20] Faulon, JL., Brown, W.M., Martin, S., "Reverse Engineering Chemical Structures from Molecular Descriptors: How Many Solutions?," Journal of Computer-Aided Molecular Design, Vol. 19, pp. 637-650, 2005.
- [21] Villaverde, A. F., Banga, J. R., "Reverse Engineering and Identification in Systems Biology: Strategies, Perspectives and challenges," Journal of the Royal Society Interface, Vol. 11, No. 91, Article No. 20130505, 2014.
- [22] Iglesias, P. A., "Systems Biology: The Role of Engineering in the Reverse Engineering of Biological Signaling," Cells, Vol. 2, No. 2, pp. 393-413, 2013.
- [23] Pan, J. B., Xu, J. Z., Zhang, C. L., "Simulation and Experimental Research of Digital Manufacturing Based on Reverse engineering," IOP Conference Series: Earth and Environmental Science, Vol. 692, Article No. 042106, 2021.
- [24] Song, Z. L., Huang, J. B., Zhang, Y. J.,

- Men,g B. G., Zhang, H., Peng, C. T., "Analysis on Wear of Sprocket Wheel Using Reverse Engineering Technology," Coal Mine Machinery. Vol. 11, pp.134-135, 2014.
- [25] Chen, Z. S., Zou, Z. C., Liu, W. L., "Innovative Design of Connecting Rod Based on Reverse Engineering Technology," Mechanical Engineer, Vol. 11, pp. 77-78, 2019.
- [26] Yu, T. B., Sun, X., Ha. D., "Structure Modeling of Artificial Bone Tissue Based on Reverse Engineering and UG Secondary Development," Modern Manufacturing Engineering, Vol. 3, pp. 154-159, 2018.
- [27] Chikofsky, E. J., Cross, J. H., "Reverse Engineering and Design Recovery: A Taxonomy," IEEE Software, Vol. 7, No. 1, 1990.
- [28] Bird, D. T., Ravindra, N. M., "A Review: Advances and modernization in U.S army gun propellants," JOM, Vol. 73, pp. 1144-1164, 2021.
- [29] Zhang, H., Xu, B., Liu, Z., Liao, X., "Effect of Nitrate Nitrogen Content on Properties of Modified Single-base Propellant," Journal of Physics: Conference Series, Vol. 1676, Article No. 012011, 2020.
- [30] Boulkadid, K. M., Trache, D., Krai, S., Lefebvre, M. H., Jeunieau, L., Dejeaifve, A. "Estimation of the Ballistic Parameters of Double Base Gun Propellants,' Propellants, Explosives, Pyrotechnics, Vol. 45, No. 5, pp. 751-758, 2020.
- [31] Wang, B. B., Liao, X., Wang, Z. S., DeLuca, L. T., Liu, Z. T., He, W. D., "Effects of Particle Size and Morphology of NQ on Thermal and Combustion Properties of Triple-base Propellants," Combustion and Flame, Vol. 193, pp. 123-132, 2018.
- [32] Zhang, F., Zhu, D. P., Liu, Q., Liu, Z. T., Du, P., "Study on the Effect of RDX Content on the Properties of Nitramine Propellant," Defence Technology, Vol. 13, pp. 246-248, 2017.
- [33] Naya, T., Kohga, M., "Influences of Particle size and Content of RDX on Burning Characteristics of RDX-based Propellant," Aerospace Science and Technology, Vol. 32, No. 1, pp. 26-34, 2014.
- [34] Naya, T., Kohga, M., "Influences of Particle size and Content of HMX on Burning characteristics of HMX-based Propellant," Aerospace Science and Technology, Vol. 27,

- No. 1, pp. 209-215, 2013.
- [35] Damse, R. S., Singh, A., Singh, H., "High Energy Propellants for Advanced Gun Ammunition based on RDX, GAP and TAGN Compositions," Propellants, Explosives, Pyrotechnics, Vol. 32, No. 1, pp. 52-60, 2007.
- [36] Wang, Z. H., Wei, C. Y., Zhu, X. B., Wang, X. B., He, J. L., Zhao, Y., "A Hierarchical Carbon Nanotube Forest Supported Metal Phosphide Electrode for Efficient Overall water splitting," Journal of Materials Chemistry A, Vol. 9, No. 2, pp. 1150-1158, 2021.
- [37] Mendonça-Filho, L. G., Rodrigues, R. L. B., Rosato, R., Galante, E. B. F., Nichele, J., "Combined Evaluation of Nitrocellulosebased Propellants: Toxicity, Performance, and Erosivity," Journal of Energetic Materials, Vol. 37, No. 3, pp. 293-308, 2019.
- [38] Al-Dhahir, T. A., Al-Mahdawi, M. E., "Dielectric and Optical Behaviors for Pure Potassium Sulfate and Doped with Copper and Iron," Iraqi Journal of Science, 2016, Vol. 57, No.3A, pp. 1699-1706.
- [39] Varghese, T. L., Krishnamurthy, V. N., The Chemistry and Technology of Solid Rocket Propellants (A Treatise on Solid Propellants), Allied Publishers Pvt. Ltd., Maharashtra, India, pp. 232-233, 2017.
- [40] Costa, M. N., Veigas, B., Jacob, J. M., Santos, D. S., Gomes, J., Baptist, P. V., Martins, R, Inacio, J., Fortunato, E., "A low Cost, Safe, Disposable, Rapid and Self-Sustainable Paper-based Platform for Diagnostic Testing: Lab-on-paper," Nanotechnology, Vol. 25, No. 9, Article No. 094006, 2014.
- [41] Celebioglu, A., Aytac, Z., Kilic, M. E., Durgun, E., Uyar, T., "Encapsulation of Camphor in Cyclodextrin Inclusion Complex Nanofibers via Polymer-free Electrospinning: Enhanced Water Solubility, High Temperature Stability, and Slow Release of Camphor," Journal of Materials Science, Vol. 53, pp.5436-5449, 2018.
- [42] Cieslak, K., Ganczyk-Specjalska, K., Drozdzewska-Szymanska, K., Uszynski, M., "Effect of Stabilizers and Nitrogen Content on Thermal Properties of Nitrocellulose Granules," Journal of Thermal Analysis and Calorimetry, Vol. 143, pp. 3459-3470, 2021.
- [43] Jia, X. L., Wei, L. X., Liu, X. W., Li, C.,

- Geng, X. H., Fu, M. M., Wang, J. G., Hou, C. Н., Xu. J., "Fabrication Characterization Submicron of Scale Spherical RDX, HMX, and CL-20 without Soft Agglomeration," Journal Nanomaterials, Vol. 2019, Article No. 7394762, 2019.
- [44] Li, X., Feng, S. L., Liu, S. Y., Li, Z. H., Wang, L., Zhan, Z. Y., Lu, W. Q., "Fabrication of ZnO Nanowires Array with Nanodiamond as Reductant," RSC Advances, Vol. 6, pp. 96479-96483, 2016.
- [45] Park, S. E., Jeong, H. T., Cho, Y. C., Jeong, S. Y., "Ferroelastic Properties of K<sub>2</sub>SO<sub>4</sub> Crystals," Journal of the Korean Physical Society, Vol. 32, pp. S786-S788, 1998.

Tsung-Mao Yang et al.

Application of Chemical Reverse Engineering on Gun Propellant Composition Analysis: A Case Study